Journal of Materials and Environmental Science
ISSN : 2028-2508
e-ISSN : 2737-890X
CODEN : JMESCN

J. Mater. Environ. Sci., 2023, Volume 14, Issue 8, Page 935-946

http://www.jmaterenvironsci.com

Photocatalytic Degradation and Kinetics of Dyes in Textile Effluent Using UV – TiO_2-W System

Effiong J. F. [1] *, Nyong A. E. [1,2], Obadimu C. [1], Udoh G. [1,**]**

[1]*Department of Chemistry, Faculty of Natural and Applied Sciences, University of Uyo, P.M.B.1515, Akwa Ibom State, Nigeria*

[2]*Department of Chemstry, Akwa Ibom State University, Mkpat Enin P. M. B. 5025, Akwa Ibom State, Nigeria*

**Corresponding author, Email address: joshuaeffiong@gmail.com*

***Corresponding author, Email address: aniedinyong@aksu.edu.ng*

Received *20 June 2023,*
Revised *05 Aug 2023,*
Accepted *08 Aug 2023*

Keywords:
- ✓ *Photocatalysis;*
- ✓ *Dyes;*
- ✓ *Textile effluents;*
- ✓ *Kinetics;*

Citation*: Effiong J. F., Nyong A. E., Obadimu C. Udoh G. (2023) Photocatalytic Degradation and Kinetics of Dyes in Textile Effluent Using UV-TiO_2-W System, J. Mater. Environ. Sci., 14(8), 935-946*

Abstract: This study investigates the photodegradation of a mixture of 4 azo dyes (direct orange 39, chlorantine fast red 5B, viscose black B and direct sky blue K) present in textile effluents and the influence of catalyst dose, irradiation time, UV power intensity and temperature on the overall photodegradation kinetics of the process. The photocatalytic experiments were conducted in a batch stirred photoreactor equipped with a 10 W, 30 W and 60 UV lamps, magnetic stirrer and thermometer. The photocatalysts used was titanium nanoparticle doped with tungsten (TiO_2: W = 93.8: 5.8, 10 nm). The results obtained showed that variation in the physical parameters influenced the efficiency of photodegradation. The kinetic study indicated that the photodegradation of the dyes present in the effluent from the textile industry followed the Langmuir-Hinshelwood model that is modified to accommodate reactions occurring at a solid-liquid interphase. At the catalyst dose of 0.5 g/l, the apparent first order rate constant K^1, was 0.00463 min^{-1} but at 2.5 g/l it reduced to 0.00338 min^{-1}. The best degradation was at the catalyst dose of 2.0 g/L with the rate constant of 0.00992 min^{-1}.

1. Introduction

Dyes and pigments are essentially those chemicals that are used to add or change the colour of materials and are widely used in the textile, pharmaceutical, food, cosmetics, plastics, paint, ink, photographic and paper industries (Khezrianjoo & Revanasidappa, 2013). It is known that about fifty percent of the world's dye consumption is within the textile industry alone (Lellis *et al.* 2019). Among the several classes of textile dyes, it is the reactive dyes that are most commonly in use with azo and anthraquinone groups being the most common chromophore groups (Lee & Pavlostathis, 2019).

There is considerable dye loss in textile waste-water during manufacturing or processing operations (Dinder & Icli, 2001; Rais *et al.* 2008). These synthetic dyes in these textiles waste-water impact adversely on life forms when discharged directly into the environment (Khezrianjoo & Revanasidappa, 2013; Galindo *et al,* 2016). The presence of sulphur, naphthol, vat dyes, nitrates, acetic acid, soaps, enzymes, chromium compounds and heavy metals in the textile waste-water make the textile effluent highly toxic (Kant, 2012; Medjahed *et al,* 2013). The colloidal matter present along with dyes increase the turbidity, thus preventing the penetration of sunlight necessary for the process

of photosynthesis within the water bodies these effluents are discharged into (Islam *et al,* 2015). This interferes and impedes the oxygen transfer mechanism useful for marine life and the self-purification process of water. Therefore, it is important to remove these dyes from the waste waters before their final disposal.

Consequently, technological systems for the removal of organic pollutants such as adsorption on activated carbon (Wang *et al,* 2014; Jodeh *et al,* 2014; Kankou *et al.* 2021), reverse osmosis (Jamil *et al,* 2020), ion exchange on synthetic resins (Davaisy *et al,* 2023), ozonation (Otieno, *et al,* 2019) and biological methods (Meena *et al,* 2021) have been developed to deal with this problem. However, most of these methods face the drawbacks of having high operational cost and lower efficiency in removing the dyes from effluents (Tien *et al,* 2022). To this end, advanced oxidation processes have been developed to circumvent these stated drawbacks and these processes are based on the generation of very reactive species that can oxidize these dyes in waste water effluents. The generated reactive species can oxidize a broad range of organic pollutants quickly and non-selectively (Qutub *et al,* 2022). Heterogeneous photocatalysts have appeared as an emerging option for the generation of reactive chemical species needed in the oxidization of environmental pollutants. This process consists of the non-selective destruction of organic compounds in the presence of ultra-violet light (UV light) and photocatalysts such as TiO_2, CdS, WO_3 and ZnO.

Among the various photocatalysts, TiO_2 has been one of the most promising material due to its non-toxicity, chemical inertness, photochemical activity and moderate cost (Qutub *et al,* 2022; Goa *et al,* 2018). However, the small surface area, poor photo response under visible light and the high rate of photogenerated electron/hole pair recombination among TiO_2 nanoparticles are the main factors limiting further improvement of its photocatalytic efficiency. Another very prominent problem associated with the use of TiO_2 is its wide band gap which limits its UV absorption ability (Konstantinou & Albanis, 2004). Many researchers are of the opinion that the photocatalytic properties of TiO_2 can be improved considerably when doped with suitable element or compound (Ekwere *et al,* 2018). Other photocatalysts have been developed that are composites in nature or are doped with other materials to improve their efficiencies. For instance, a composite assembled from nano zinc oxide (ZnO) and nanocellulose has been used as a photocatalyst in the degradation of congo red dye (Jamal *et al,* 2020). In the same vein, a study has reported the synthesis and evaluation of the mixed metal oxides MgO/Al_2O_3-TiO_2 and ZnO/Al_2O_3-TiO_2 as heterogeneous photocatalysts for the photodegradation of a mixture of organic dyes such as methylene blue and methyl orange (Castro *et al,* 2021). Similar works but with different types of photocatalysts, mostly in the form of doped nanoparticles or composites have been reported in literature (Yadav *et al,* 2022; Diyana *et al,* 2019; Nathan *et al,* 2019; Nyong *et al,* 2022).

Consequently, the objective of this work is to study or investigate the kinetics, influence of various physical parameters (irradiation time, catalyst loading, light intensity and temperature) on the photocatalytic mineralization of dyes in actual textile effluent, in the presence of TiO_2 doped with tungsten, irradiated by the UV light in a batch stirred reactor. TiO_2 doped with tungsten is actually a novel photocatalyst whose capacity at photodegradation and the kinetics of such photodegradation of a typical textile effluent has not been studied.

2. Methodology

2.1 Sourcing and preparation of samples for the experiments

The materials that were used for these experiments include titanium dioxide doped with tungsten (TiO_2-W) nanoparticles. The TiO_2-W nanoparticles was obtained from US Nano Incorporated, with

the average size of 10 nm as well as 99.99 % purity. It consisted of 93.8 weight percent of TiO_2 (anatase) and 5.8 weight percent Tungsten (W). This TiO_2-W nanoparticles was used as the photocatalyst without further treatment. The textile effluent, consisting of dyes, was obtained from SAVCO Garments and Printers, Aba in Abia State, Nigeria and it was also used directly without any further processing. The photocatalytic degradation of the effluent dyes was effected in a rectangular batch stirred reactor with a capacity of 150 cm^3. This reactor has an inserted thermometer to monitor the temperature, a magnetic stirring mechanism and UV lamps, placed 5 cm from the sample. The ultra-violet (UV) lamps (manufactured by Sandiz Energy Limited) used had 10 W, 30 W and 60 W power rating. For the ultra-violet spectrophotometric analysis, the UV-Vis spectrophotometer (Labomed 1286 series) was used. High Performance Liquid Chromatography (HPLC) Enhanced Integrator was used to determine the components of the dye effluent and their concentration.

2.2 Experiments

2.2.1 Evaluation of the chemical composition of the textile effluent

We used the High-Performance Liquid Chromatographic technique to evaluate the chemical constituents of the textile effluents that was obtained from SAVCO Garments and Printers.

2.2.2 Photodegradation test (photolysis)

50 ml of the textile effluent was introduced into the photocatalytic reactor and was stirred continuously with a magnetic stirrer for 30, 60, 90, 120 and 180 minutes respectively under UV light irradiation. After these specified time frames of exposure of the textile effluent to UV-irradiation, some of the effluent samples were analyzed via the UV spectrophotometer to determine the dye concentration.

2.2.3 Procedure for dark reaction in presence of the TiO_2-W nanoparticles

50 ml of the effluent mixed with 0.1 g of TiO_2-W nanoparticles was again introduced into the photocatalytic reactor and this suspension was further agitated in the dark by means of magnetic stirring for 30, 60, 90,120 and 180 minutes respectively. The resultant dye suspension was filtered and the suspended photocatalyst removed. The remaining effluent solutions were analyzed using the UV spectrophotometric technique, to determine if there were any changes in the concentrations of the chemical constituents. The differences in concentrations (before and after the adsorption test) was attributed to the photodegradation of the dyes by the photocatalyst.

2.2.4 Procedure for photocatalytic degradation of the textile effluent

50 ml each of the effluent was mixed with 0.1 g of TiO_2-W in the photocatalytic reactor, as done previously in 2.2.3. The suspension was continuously stirred magnetically while being irradiated by the ultra-violet light from ultra-violet lamps rated at 10 W, 30 W and 60 W respectively. This irradiation was done at room temperature. Aliquots of the mixture (5 ml) were centrifuged, filtered and analyzed periodically at 0, 30, 60, 90, 120, 150, and 180 minutes respectively. The degradation process again was monitored via the UV spectrophotometric technique. The percentage degradation of the dyes present in the effluent with respect to its initial concentration at any time can be obtained from **Eqn. 1**.

$$x = \frac{C_o - C}{C_o} * \frac{100}{1} \qquad \textbf{Eqn. 1}$$

where C_o and C are the initial and final concentrations at a given time.

3. Results and Discussion

The results obtained from these experimental procedures are presented and discussed as follows.

3.1 Chemical Composition of Textile Effluent

The results of the HPLC performed on the textile effluent are stated in **Table 1**. The textile effluent was found to consist of Direct Orange 39, Chlorantine Fast Red 5B, Viscose Black G and Direct Sky-Blue K dyes. The dominant dye in the effluent is Chlorantine Fast Red 5B. The reddish colour of the textile effluent is therefore due to the dominance of Chlorantine Fast Red 5B in its composition.

Table 1. The chemical composition of textile effluent from SAVCO Garments and Printers, Nigeria

Chemical Composition	Amount (mg/l)
Direct orange 39	3.20
Chlorantine fast red 5B	6.06
Viscose black G	0.31
Direct sky blue K	1.64
Total	11.21

A total concentration of the dyes is determined by the addition of the amounts, in mg/l, of these various dyes that were identified by the HPLC analysis and the value of 11.21 mg/l was obtained. This value is lower than the standard textile effluent concentration (30-50 mg/l) (Konstantinou & Albanis, 2004).

3.2 Working Curve

In order to determine the changes in the concentration of the dyes in the effluent, during the course of our experiments, a working curve which is presented in **Figure 1** was generated with standard concentrations of the effluent.

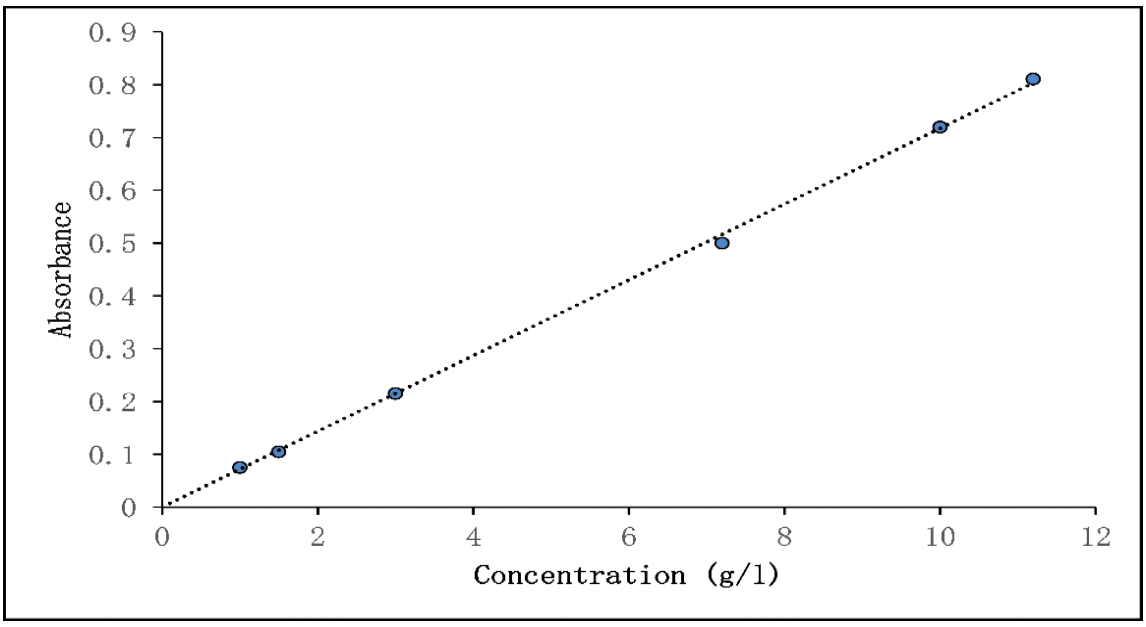

Figure 1. Calibration curve of the dye's concentration (mg/l) (Wavelength of absorbance at 510 nm)

3.3 Effect of only UV irradiation on the Textile Effluent

The changes in the concentrations of the various dyes that constitutes the textile effluent are presented in the **Table 2**. These changes in the concentrations are due only to the UV irradiation action

as there was no photocatalyst present. As can be seen in **Table 2**, there was only a small decrease in the concentrations. In this case, the concentration of the dyes in the textile effluent decreased from an initial concentration of 11.21 mg/l to a final concentration value of 11.0 mg/l after 3 hours, indicating 1.80 % removal of the dyes when the TiO_2-W nanoparticles photocatalyst was absent.

3.4 Effect of TiO_2-W nanoparticles on the Dyes present in the Textile Effluent in the absence of UV-light Irradiation

With TiO_2-W nanoparticles dose of 2.0 g/l, the level of degradation in the absence of UV irradiation was still insignificant as can be seen in **Table 2**. The TiO_2-W nanoparticles only caused the dyes to degrade from an initial total concentration value of 11.21 mg/l to 10.68 mg/l when the experiments were done in the dark, in the absence of UV irradiation. This implied that only 5% of the dyes were removed after 180 minutes of exposing the effluents to the TiO_2-W nanoparticles only. Therefore, the processes explained in sections 3.3 and 3.4 played limited, inconsequential roles in the degradation and mineralization of the dyes contained in the effluent.

Table 2: Variation of concentration and degradation efficiency with time during photolysis and dark experiment

Time (mins.)	Final concentration (without TiO_2-W)	Final concentration (without UV light)	% degradation (without TiO_2-W)	% degradation (without UV light)
0	11.21	11.21	0.00	0.00
30	11.10	11.05	0.90	1.42
60	11.10	11.05	0.90	1.42
90	11.00	10.90	1.80	2.76
120	11.00	10.70	1.80	4.54
180	11.00	10.68	1.80	4.72

3.5 Effect of Irradiation Time

Under the experimental conditions, 71.5% of the dye mineralized within 120 minutes of irradiation. The effect of the time of UV irradiation of the effluent is presented in **Table 3** where the % degradation of the dyes in the effluent at the different irradiation periods of 30, 60, 90, 120 and 180 minutes are expressed. These values were obtained for the optimum photocatalyst loading of 2.0 g/l. The photocatalytic degradation of the dyes occurs on the surface of TiO_2-W nanoparticles that served as a photocatalyst. In this case, oxygen and hydroxyl radicals are trapped in the holes present on the nanoparticles surfaces on which the dyes present in the effluent are adsorbed. These radicals are strong enough to break the bonds of the dyes' molecules resulting in their degradation (Saien *et al,* 2008).

When the intensity of light and concentration of dye are constant, it is known that the number of radicals increase with increase irradiation period. As the irradiation time increases, several intermediate products are formed due to fragmentation of the dyes' molecules. These intermediates undergo degradation on further irradiation (Mathews, 1990). For the irradiation periods of 0, 30, 60, 90, 120 and 180, the concentrations of the dyes in the effluent decreased from an initial concentration of 11.2 mg/l to 7.20, 6.10, 4.51 and 3.20 mg/l for the corresponding irradiation periods respectively. This corresponded to the percent degradation efficiencies of 35.7, 45.5, 59.7 and 71.5 %. It should be noted that there was no change in the concentration of dyes when the irradiation time increased above 120 minutes. This may be due to opacity problem caused by too many fragmented molecules, preventing further penetration of UV light into the suspension (Neena *et al,* 2018). **Figure 2** shows the variation of the percent degradation efficiencies of the dyes as a function of the irradiation time.

3.6 Effect of TiO_2-W Photocatalyst Concentration

The variation of the concentration and the % degradation of the dyes in the textile effluent with the amount of TiO_2-W photocatalyst showed that as the amount of the TiO_2-W increased, the concentration of the dyes in the effluent reduced, with attendant increase in the % degradation efficiency. Using 0.5, 1.0, 1.5, 2.0 and 2.5 g/l as the concentration of the photocatalyst, concentration of the dyes in the effluent varied from its initial concentration of 11.21 mg/l to 6.3, 5.4, 4.0, 3.2 and 7.5, respectively. This corresponded to the degradation efficiencies of 43.8%, 51.8%, 64.3%, 71.5% and 33.0% as depicted in **Figure 3**.

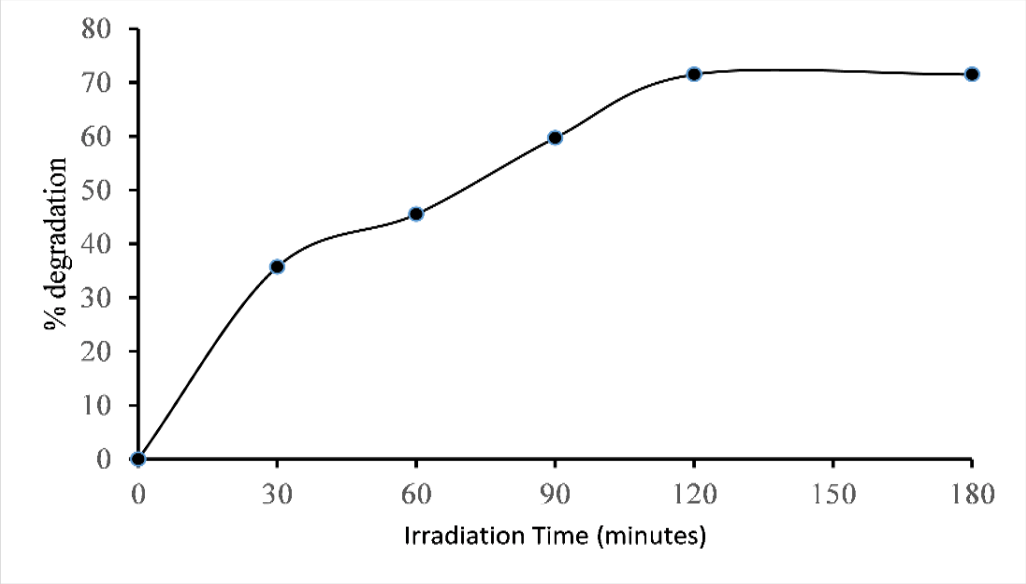

Figure 2. Effect of irradiation times on degradation of the dyes. UV = 30 W, catalyst concentration = 2.0 g/l, pH = 10.7, initial dye concentration = 11.21 mg/l

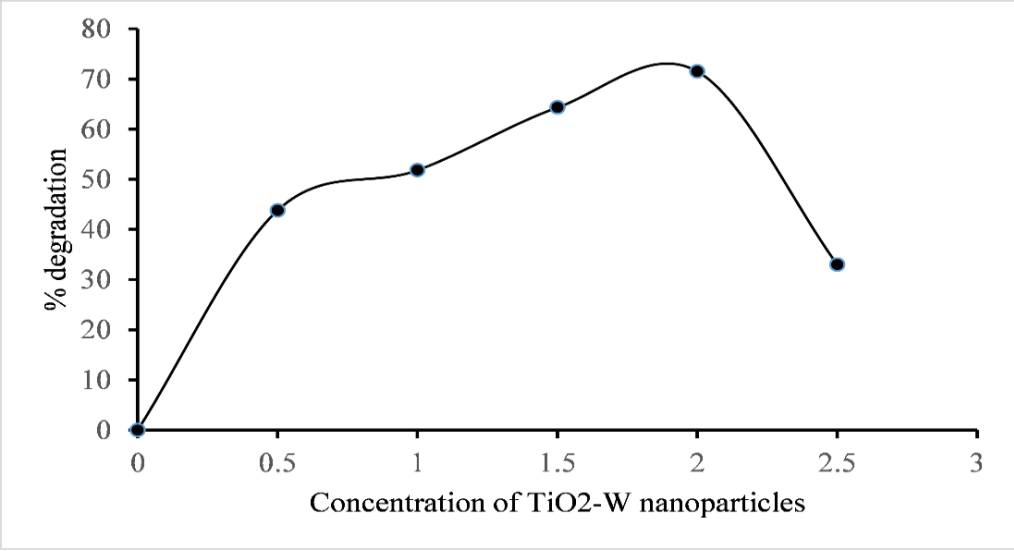

Figure 3. Effect of the amount of TiO_2-W on the degradation of dyes in textile effluent at irradiation time of 180 min, dyes concentration 11.21 mg/l, UV=30 W, pH=10.7

The percent photodegradation efficiency increased with the increase in the amount of photocatalyst until 2.0 g/l and then decreases sharply. As stated earlier, this increase is due to the availability of more active sites for photocatalysis due to the higher concentration of TiO_2-W nanoparticles. This causes

enhancement in the hydroxyl and oxygen radical generation and which also led to the increase in the degradation power because the greater number of the dye molecules could be absorbed on catalyst surface. Equally, photocatalyst concentration above 2.0 g/l results in enhancement of opacity which causes a reduction in the UV light penetration throughout the solution and a drop in the percent degradation efficiency (Lee et al, 2015).

3.7 Effect of UV Power Intensity

Due to the fact that the dye decomposition is a heterogeneous reaction occurring on the TiO_2-W particle surface with the active site concentration increasing with the UV energy received, a higher UV power intensity is expected to give a higher decomposition rate (Valente et al, 2006). A series of experiments were conducted under the same operating conditions but varying UV power intensities and the results are shown in **Table 3**. The interception of more light provides increased adsorption of the light on the photocatalyst surface thereby making the surface more active. The simple implication of this is that as the power rating of the UV light source increased, the capacity of the light to trigger the creation of reactive species within the system increased. As can be seen in **Figure 4**, the decrease in the concentration of the dyes in the effluent was least when the light source was 10 W and most when the light source used was 60 W. For the duration of 180 minutes in which this experiment was carried out, the concentration of the dyes in the textile effluents changed from its initial value by 0.023 mg/l per minute, 0.044 mg/l per minute and 0.051 mg/l per minute when the UV power source used were 10 W, 30 W and 60 W respectively.

Table 3: The concentration of the dyes in the textile effluent at different irradiation times under 10 W, 30 W and 60 W UV light source

Time (m)	10 W UV source Concentration (mg/L)	30 W UV source Concentration (mg/l)	60 W UV source Concentration (mg/L)
0	11.2	11.2	11.2
30	10.6	7.2	6.6
60	9.4	6.1	5.2
90	8.1	4.5	3.3
120	7.0	3.2	2.2
180	7.0	3.2	2.1

3.8 Effect of Temperature

From the experiments carried out under the same operating conditions but varying reaction temperatures, the following results were obtained as shown in **Table 4**. The dye decomposition rate increases with the temperature. This presented graphically in **Figure 5**. A higher temperature will give a faster decomposition rate because at higher temperatures, the activation energies of the dye reaction and the UV penetration through the dye solution are positive (Valente et al, 2006). This means that a higher temperature favors the dye degradation reaction and UV penetration. Also, at higher temperatures, the heat of adsorption of the dye molecules onto the TiO_2-W particle is more exothermic meaning a lower free energy. This enhances the overall rate of degradation. In addition, at high temperature, mobility of holes and electrons are enhanced.

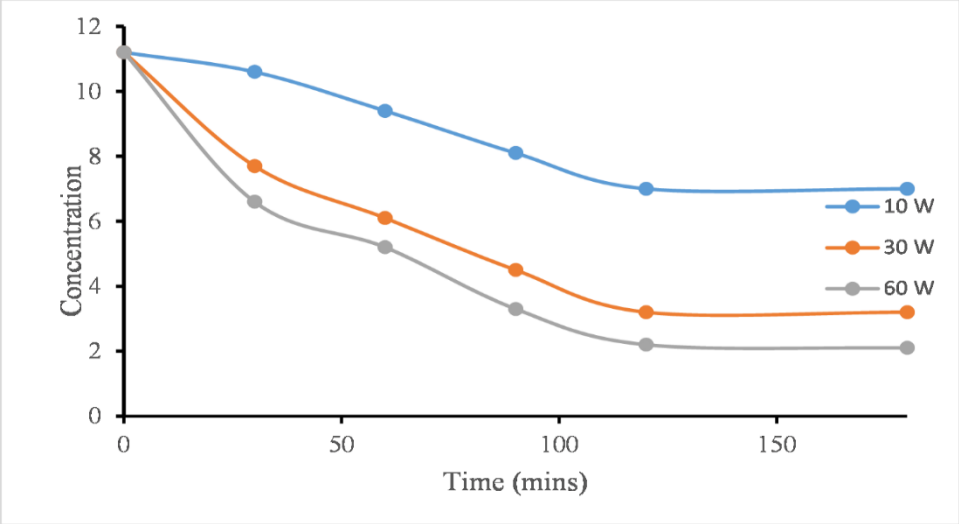

Figure 4. Effect of UV irradiation of different intensities on the degradation of the dyes in the textile effluent. Initial dye concentration in textile effluent = 11.21 mg/l, optimum TiO_2-W concentration = 2.0 g/l

Table 4. Variation of concentration of dyes with time at different temperature

Time (min.)	Concentration (mg/l) at 30 ^{0}C	Concentration (mg/l) at 40 ^{0}C	Concentration (mg/l) at 60 ^{0}C
0	11.2	11.2	11.2
30	8.0	7.8	6.9
60	4.5	4.5	3.9
90	2.8	2.6	2.0
120	2.5	2.3	1.8
150	2.5	2.5	1.9
180	2.5	2.5	1.9

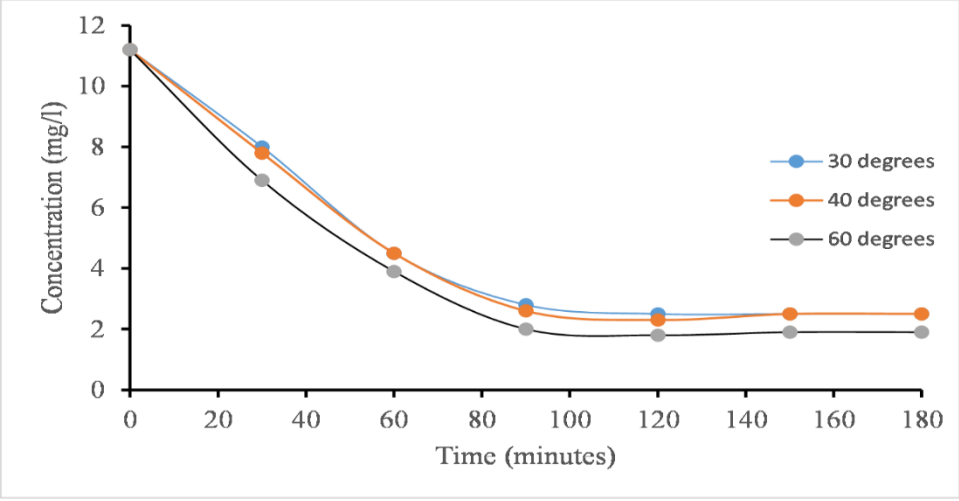

Figure 5. Effect of degradation temperature on the dye concentration

3.9 Kinetics of Degradation of Dyes in Textile Effluent

The kinetics of the photocatalytic degradation of many organic compounds in suspensions of photocatalysts under illumination has been modeled using the equation of Langmuir-Hinshelwood (Ad *et al,* 2016; Valente *et al,* 2006). This model considers that the reaction rate is proportional to the photocatalyst surface fraction covered by the substrate as shown in **Eqn. 2 & 3**:

$$r = \frac{-dC}{dt} = k\theta \qquad \textbf{Eqn. 2}$$

$$\theta = \frac{K_1 C}{1+K_1 C} \qquad \textbf{Eqn. 3}$$

where k is the kinetic constant, K_1 is the constant of the reactant adsorption on the surface of the photocatalyst and C is the concentration of the dye solution in mol/litre.

Substituting **Eqn. 2** in **Eqn. 3** yields:

$$r = \frac{-dC}{dt} = \frac{KK_1 C}{1+ K_1 C} \qquad \textbf{Eqn. 4}$$

Integrating **Eqn. 4**:

$$In\left(\frac{C_0}{C}\right) + K_1(C_o - C) = KK_1 t \qquad \textbf{Eqn. 5}$$

where t is the irradiation time and C_o is the initial concentration.

Eqn. 5 is zero order when the concentration C (mol/l) is high but when the solution is diluted the reaction is an apparent first-order reaction with an apparent kinetic constant of a pseudo first order reaction as shown in **Eqn. 6**.

$$r = \frac{-dC}{dt} = KK_1 C \qquad \textbf{Eqn. 6}$$

Integrating **Eqn. 6**, we have:

$$-\int_{C_o}^{C} \frac{dC}{C} = \int_0^t K_{ap}\, dt \qquad \textbf{Eqn. 7}$$

$$In\left(\frac{C_0}{C}\right) = K_{ap} t \qquad \textbf{Eqn. 8}$$

Plotting $In\left(\frac{C_0}{C}\right)$ versus t, it is possible to determine the apparent kinetic constant. The plot gives a straight line, and its slope from linear regression represents the value of K_{ap}. This approach is considered as the main path for evaluating dye degradation kinetics.

The regression analysis of the variation of the natural logarithm of the normalized concentration of the dye effluent with the irradiation time, gave a good approximation over the range of 0.5 g/l to 2.5 g/l catalyst concentration within the period of 120 minutes. Considering that our kinetic model represents a pseudo first-order reaction, we can evaluate the half-life from the relationship given in **Eqn. 8**.

The increase in the TiO_2-W loading from 0.5 g/L to 2.0 g/L increased the apparent rate constant from 0.004635 to 0.00992. Beyond this optimal dose, K_{ap} values decreased. These values for the K_{ap}, R^2, from the regression analysis and r_o are presented in **Table 5**. This can be rationalized in terms of availability of active sites on the TiO_2-W surface and the penetration of photoactivating light into the suspension. The availability of active sites increases with catalyst loading, but the light penetration and hence the photoactivated volume of the suspension shrinks (Hegyi *et al,* 2023; Sleiman *et al,* 2007).

Table 5: The calculated values of K_{ap}, half-life ($t_{\frac{1}{2}}$), regression coefficient (R^2), and the rate of degradation (r_o)

Concentration of TiO_2-W	K_{ap} (min-1)	half-life ($t_{\frac{1}{2}}$), (min)	R^2	r_o (mg/min)
0.5	0.004635	149.5	0.9976	0.05191
1.0	0.007293	95.0	0.9699	0.08168
1.5	0.007805	88.7	0.9767	0.08742
2.0	0.00992	69.8	0.9951	0.11111
2.5	0.003384	204.4	0.9996	0.03790

The trade-off between these two effects is that at low solution concentration, when there are excess active sites, the balance between the opposing effects is evenly poised and change in photocatalyst loading makes little difference on the rate of degradation (Shaw *et al,* 2011). At high catalyst concentration, availability of excess active sites outweighs the diminishing photoactivated volume and significantly greater rate of degradation is achieved at increased TiO_2-W loading. The decreased value at higher catalyst loading may be due to the deactivation of activated molecules by collision with ground state molecules (Shankar *et al,* 2003; Erdemoğlu *et al,* 2008; Lee *et al,* 2022; Effiong *et al*, 2023).

Conclusion

In conclusion, the degradation efficiency of the TiO_2-W photocatalyst with respect to the textile effluent was 71.5% under optimum experimental conditions. It was found that the catalyst loading, irradiation time, temperature and UV power intensity influenced the photodegradation process. Generally, it was observed that the mineralization process of the effluent followed the pseudo-first-order-kinetics as confirmed by their high correlation, R^2 values. The apparent first order rate constant, increases as the catalyst loading increases. Catalyst loading beyond 2.0 g/L witnessed a reduction in the value of K_{ap}.

Disclosure statement: *Conflict of Interest:* The authors declare that there are no conflicts of interest.
Compliance with Ethical Standards: This article does not contain any studies involving human or animal subjects.

References

Ad C., Benalia M., Djedid M., Elmsellem H., Ben Saffedine F., Messaoudi A., Kadmi Y., Ouzidan Y., Hammouti B. (2016), A new lignocellulosic material based on Luffa cylindrica for Nickel(II) adsorption in aqueous solution, *Mor. J. Chem.* 4(4), 1096-1105

Castro, L. V., Ortíz-Islas, E., Manríquez, M. E., Albiter, E., Caberra-Sierra, R., Alvarado Zavala, B. (2021). Photocatalytic degradation of mixed dyes in aqueous phase by MgAlTi and ZnAlTi mixed oxides, *Topic in Catalysis*, 64, 97-111. https://DOI:10.1007/s11244-020-01345-5

Devaisy, S. Kandasamy, J., Aryal, R., Johir, M., Ratnaweera, H., Vigneswaran, S. (2023). Removal of Organics with Ion-Exchange Resins (IEX) from Reverse Osmosis Concentrate, *Membranes*, 13 (2), 136-. https://doi.org/10.3390/membranes13020136

Dinder, B. and Icli, S. (2001). Unusual photoreactivity of zinc oxide irradiated by concentrated sunlight, *Journal of Photochemistry and Photobiology A*., 140 (3), 263-268. https://DOI:10.1016/S1010-6030(01)00414-2

Diyana, N., Zambri, S., Izza Taib, N., Abdul Latif, F., Mohamed, Z. (2019). Utilization of neem leaf extract on biosynthesis of iron oxide nanoparticles, *Molecules*, 24 (20), 1-12 doi:10.3390/molecules24203803

Effiong, J. F., Nyong, A. E., Boekom, E. J., Simon, N. (2023). Photocatalytic Degradation and Kinetics of Dyes in Textile Effluent Using UV – ZnO-Al System*, Asian Journal of Applied Chemistry Research*, 13, 23-32.

Ekwere, I., Horsfall, M., Otaigbe, J. (2018). Photocatalytic degradation and kinetics of malachite green using UV-TiO_2 system, *International Journal of Engineering and Science,* 7, 42 – 51.

Erdemoğlu S., Aksu S. K., Sayılkan F., İzgi B., Asiltürk M., Sayılkan H., Frimmel F., Güçer Ş. (2008), Photocatalytic degradation of Congo Red by hydrothermally synthesized nanocrystalline TiO2 and identification of degradation products by LC–MS, Journal of Hazardous Materials, Volume 155, Issue 3, 2008, Pages 469-476, ISSN 0304-3894, https://doi.org/10.1016/j.jhazmat.2007.11.087

Galindo, G., Jacaves, P., Kait, A. (2016). Microbial removal of selected volatile organic compounds from the model landfill gas, *Chemosphere*, 23 (2), 215-228. https://DOI10.1515/eces-2016-0014

Gao, D., Wang, C., Jian, Y., Dong, P. (2018). Performance of nano-Co_3O_4/peroxymonosulfate system: Kinetics and mechanisms study using Acid Orange 7 as a model compound, *Material science*, 180 (1-2), 116-121. https://doi.org/10.1016/j.apcatb.2007.11.009

Hegyi A., Lăzărescu A.V., Ciobanu A.A., Ionescu B.A., Grebenişan E., Chira M., Florean C., Vermeşan H., Stoian V. (2023) Study on the Possibilities of Developing Cementitious or Geopolymer Composite Materials with Specific Performances by Exploiting the Photocatalytic Properties of TiO2 Nanoparticles. *Materials (Basel).* 16(10), 3741. doi: 10.3390/ma16103741

Islam, M. D., Mehedy, E., Chowdhury, S. Sen, P., Shormi, H. J., Biswas, M. (2015). Physicochemical analysis of textile dye effluent and screening the textile dye degrading microbial species*, IOSR Journal of Environmental Science, Toxicology and Food Technology*. https://DOI:10.9790/2402-09325155

Jaafar, A., Boussaoud, A., Azzaoui K., Mejdoubi, E., Chetouani, A., Hammouti, B., Berrabah, M., Lamhamdi, A. (2016). Decolorization of Basic Red 5 in aqueous solution by Advanced Oxidation Process using Fenton's reagent, *Morrocan Journal of Chemistry*. 4, 759-763

Jamal, N., Radhakrishnan, A., Raghavan, R., Bhaskaran, P. (2020). Efficient photocatalytic degradation of organic dye from aqueous solutions over zinc oxide incorporated nanocellulose under visible light irradiation, *Catalysis*, 43 (1), 84-91. https://doi.org/10.1515/mgmc-2020-0009.

Jamil, S., Loganathan, P., Kandasamy, J., Listowski, A., McDonald, J. A, Khan, S. J., Vigneswaran, S. (2020). Removal of organic matter from wastewater reverse osmosis concentrate using granular activated carbon and anion exchange resin adsorbent columns in sequence, *Chemosphere*, 261, 127549. https://doi.org/10.1016/j.chemosphere.2020.127549

Jodeh S., Basalat N., Abu Obaid A., Bouknana D., Hammouti B., Hadda T. B., Jodeh W., Warad I. (2014), Adsorption of some organic phenolic compounds using activated carbon from cypress products, *J. Chem. Pharmac. Res.*, 6 N°2, 713-723

Kankou M. S.'A., N'diaye A. D., Hammouti B., Kaya S. and Fekhaoui M. (2021) Ultrasound-assisted adsorption of Methyl Parathion using commercial Granular Activated Carbon from aqueous solution, *Mor. J. Chem.* 9(4), 832-842

Kant, R. (2012). Textile dyeing industry an environmental hazard, *Natural Science*, 4, 22-26 https://10.4236/ns.2012.41004.

Khezrianjoo S. and Revanasidappa, H. (2013). Photocatalytic degradation of acid yellow 36 using zinc oxide photocatalyst in aqueous media, *Journal of Catalysis*, 2013, 1-7. https://doi.org/10.1155/2013/582058.

Konstantinou J. K. and Albanis T. A. (2004). TiO_2-assisted photocatalytic degradation of azo dyes in aqueous solution: kinetic and mechanistic investigations, *Applied Catalysis*, 49 (1), 1-14. https://doi.org/10.1016/j.apcatb.2003.11.010

Lee, K. M., Abd Hamid, S. B., Lai, C. W. (2015). Mechanism and kinetics study for photocatalytic oxidation degradation: a case study for phenoxyacetic acid organic pollutant, *Journal of Nanomaterials.* 2015, 1-10. https://doi.org/10.1155/2015/940857

Lee, S. Y., Kang, D., Jeong, S., Do, T. H., Kim, J. H. (2022). Photocatalytic degradation of Rhodamin B dye by TiO_2 and gold nanoparticle supported on a polydimethyl siloxone sponge under UV light, *American Chemical Society*, 5 (8), 4233-4241. https//doi: 10.1021/acsomega.9b04127

Lee Y. H. and Pavlostathis S. G. (2004). Decolorization and toxicity of reactive anthraquinone textile dyes under methanogenic conditions, *Water Research*, 38 (7), 1838-1852. doi:10.1016/j.watres.2003.12.028

Lellis, B., Fávaro-Polonio, C., Pamphile, J., Polonio, J. (2019). Effects of textile dyes on health and the environment and bioremediation potential of living organisms, *Biotechnology Research and Innovation*, 3 (2), 275-290. https://doi.org/10.1016/j.biori.2019.09.001

Matthew, R. W. (1990). Purification of water with near-UV illuminated suspensions of titanium dioxide, *Water Research*, 24 (5), 653-660. https://doi.org/10.1016/0043-1354(90)90199-G

Medjahed, K., Tennouga, L., Mansri, A., Chetouani, A., Hammouti B., Desbrières, J. (2013), Interaction between poly(4-vinylpyridine-graft-bromodecane) and textile blue basic dye by spectrophotometric study, *Res. Chem. Intermed.,* 39(7), 3199-3208.

Meena, M., Sonigra, P., Yadav, D. G. (2021). Biological-based methods for the removal of volatile organic compounds (VOCs) and heavy metals, *Environmental Science and Pollution Research*, 28, 2485–2508 https://doi.org/10.1007/s11356-020-11112-4

Nathan, V., Ammini, P., Vijayan, J. (2019). Photocatalytic degradation of synthetic dyes using iron (III) oxide nanoparticles (Fe_2O_3-Nps) synthesised using *Rhizophora mucronata, IET Nanobiotechnology*, 13 (2), 120–123. https://doi: 10.1049/iet-nbt.2018.5230

Neena, D., Kondamareddy, K. K., Bin, H., Lu, D., Kumar, P., Dwivedi, R. K., Pelenovich, V., Zhao, X., Gao, W., Fu, D. (2018). Enhanced visible light photodegradation activity of RhB/MB from aqueous solution using nanosized novel Fe-Cd co-modifed ZnO, *Scientific Reports*, 10691 (2018), 1-12 https://doi.org/10.1038/s41598-018-29025-1

N'Guettia K. R.., Aboua K. N., Soro D. B., Traore K. S. (2023). Photocatalysis of dioxide for the degradation of ciprofloxacin in an aqueous medium, *Journal of Materials and Environmental Science*., 14 (3), 337-347.

Nyong, A. E., Udoh, G., Awaka-Ama, J. J, Nsi, E. W, Rohatgi, P. K. (2022). A Study of the Morphological Changes and the Growth Kinetics of the Oxides Formed by the High Temperature Oxidation of Cu-32.02% Zn-2.30% Pb Brass, *Materials Research*, 25, 1-6. https://doi.org/10.1590/1980-5373-MR-2021-0173

Otieno, B., Apollo, S. Kabuba, J., Naidoo, B., Simate, G., Ochieng, A. (2019). Ozonolysis pre-treatment of waste activated sludge for solubilization and biodegradability enhancement, *Journal of Environmental Chemical Engineering*, 7(2), 102945. https://doi.org/10.1016/j.jece.2019.102945

Qutub, N., Singh, P., Sabir, S., Sagadevan, S., Oh, W. (2022). Enhanced photocatalytic degradation of acid blue dye using Cds/TiO_2 nanocomposite, *Science Report*, 5759 (2022), 1-18. https://doi.org/10.1038/s41598-022-09479-0

Rais Z., Taleb M., Sfaira M., Filali Baba M., Hammouti B., Maghnouj J., Nejjar R., Hadji M. (2008), Decolouration of textile's effluents discoloration by adsorption in static reactor and in dynamic reactor on the phosphocalcic apatites, *Phys. Chem. News,* 38, 106-111.

Saien, J., and Khezrianjoo, S. (2008). Degradation of the fungicide carbendazim in aqueous solutions with UV/TiO_2 process: Optimization, kinetics and toxicity studies, *Journal of Harzadous Materials*, 157 (2-3), 269 -276. https://doi.org/10.1016/j.jhazmat.2007.12.094

Shankar, M. V., Neppolian, B., Sakthivel, S., Arabindoo, B., Palanichamy, M., Murugesan, V. (2003). Solar photocatalytic degradation of Azo dye: comparison of photocatalytic efficiency of ZnO and TiO_2, *Indian Journal of Engineering and Material Sciences*, 77 (1), 65-82. https://DOI:10.1016/S0927-0248(02)00255-6

Shaw, B., LucaCiceri, N., Bianchi, C.L., Grieser, F., Ashokkumar, M. (2011). Sonophotocatalytic degradation of 4-chlorophenol using Bi_2O_3/$TiZrO_4$ as a visible light responsive photocatalyst, *Ultrasonics Sonochemistry*, 18 (1), 135-139. https://doi.org/10.1016/j.ultsonch.2010.04.002

Sleiman, M., Vildozo, D., Ferronato, C., Chovelon, M. (2007). Photocatalytic degradation of azo dye Metanil Yellow: Optimization and kinetic modeling using a chemometric approach, *Applied Catalysis B,* 77 (1-2), 1-11. https://doi.org/10.1016/j.apcatb.2007.06.015

Tien, T. M., Chen, C. H., Huang, C. T., Chen, E. L. (2022). Sensing performance of precisely ordered TiO_2 nano wire, *Catalysts*, 13 (1), 865–874. https://doi.org/10.3390/s130100865

Valente, J.P., Padilha, P.M., Florentino, A.O. (2006). Studies on the adsorption and kinetics of photodegradation of a model compound for heterogeneous photocatalysis onto TiO_2, *Chemosphere*, 67 (7), 1128-1133. https://doi.org/10.1016/j.chemosphere.2005.11.050

Wang, J., Wang, R., Ma, J., Sun. Y. (2014). Study on the Application of Shell-Activated Carbon for the Adsorption of Dyes and Antibiotics, *Water*, 14(22), 3752-. https://doi.org/10.3390/w14223752

Yadav, S., Shakya, S., Singh, K., Gupta, D. (2022). A review on degradation of organic dyes by using metal oxide semiconductors, *Environmental Science and Pollution Research.* 30, 71912–71932. https://doi.org/10.1007/s11356-022-20818-6